Low hormetic dose of curcumin-PDA nanoparticles improves viability and proliferation in cell culture

Vázquez Alberdi, L.[1,2]; Martínez-Busi, M.[3]; Echeverry, C.[4]; Calero, M.[5]; Kun, A.[1,6]

1- Laboratorio de Biología Celular del Sistema Nervioso Periférico, Departamento de Proteínas y Ácidos Nucleicos, Instituto de Investigaciones Biológicas Clemente Estable, Montevideo 11600, Uruguay; lvazquez@iibce.edu.uy
2- Laboratorio de Acústica, Instituto de Física, Facultad de Ciencias, Universidad de la República, Montevideo 11400, Uruguay
3- Plataforma Química Analítica, Instituto de Investigaciones Biológicas Clemente Estable, Montevideo 11600, Uruguay; mmartinez@iibce.edu.uy
4- Departamento de Neurobiología y Neuropatología, Instituto de Investigaciones Biológicas Clemente Estable, Montevideo 11600, Uruguay; cecheverry@iibce.edu.uy
5- Unidad de Encefalopatías Espongiformes, UFIEC, CIBERNED, Instituto de Salud Carlos III,28029 Madrid, Spain; mcalero@isciii.es
6- Sección Bioquímica, Facultad de Ciencias, Universidad de la República, Montevideo 11400, Uruguay; akun@fcien.edu.uy

Corresponding author: Kun, A. akun@fcien.edu.uy, Tel.: +598-2487-1616; Fax: +598-2487-5461

Abstract:

Curcumin is a polyphenol extracted from the roots of the Curcuma longa plant. Low doses of curcumin are related to anti-inflammatory, antioxidant and neuroprotective effects, while high doses are used for their lethality. This diversity of behaviors allows us to understand curcumin as a compound with hormetic action. Due to its hydrophobic character, curcumin is solubilized in organic compounds, about which we have recently reported undesirable effects on the viability and proliferation of primary cultures of Schwann cells. The use of nanoparticles as delivery systems has been shown to be a successful strategy for many compounds. In the present work we describe the structure of Polydopamine (PDA) nanoparticles, loaded or not with a low dose of curcumin (0.05 µM), which we characterized by transmission and scanning electron microscopy. We analyzed the curcumin-PDA turnover with UHPLC-MS, and describe two different hydrophobic forms of curcumin, released at different times from their PDA-carrier. An increased cell viability and proliferation was observed in endoneurial fibroblast primary cell culture, when a low dose of curcumin-PDA was steadily supplied by prolonged periods. Furthermore, PDA alone as a vehicle showed no effect on viability and proliferation, in the same conditions. These results confirm the beneficial properties of curcumin at very low doses, thus widening its therapeutic window thanks to the increased bioavailability provided by our biological approach.

Keywords: Curcumin; Polydopamine-Nanoparticles; Hormesis; Viability; Proliferation.

1. Introduction

Curcumin is a polyphenol extracted from the roots of the *Curcuma longa* plant, native to India [1–4]. It is a yellow-orange solid that has diverse applications, with a broad spectrum of action depending on both its concentration and the time of administration [5–12]. It has been reported that low doses of curcumin are related to anti-inflammatory [13,14], antioxidant [9,15–17], and neuroprotective effects [10,11,18,19]; whereas, at high concentrations, it has lethal effects, which is why it is used as a potent anti-tumor agent [5–8,20,21]. This diversity of behaviors allows us to understand curcumin as a hormetic compound. Thus, at low doses it has cellular effects that promote cell development, while at high doses it promotes cell death, being used for its anti-tumor properties [22–24].

Due to its hydrophobic character, curcumin needs to be solubilized in organic solvents, the most conventionally used being ethanol and dimethyl sulfoxide (DMSO) [20,21,25–28]. Unfortunately, these vehicles present effects by themselves (especially visible at prolonged exposure times), more or less detectable depending on the biological models used [29–32]. Recently, we have reported effects on the viability and proliferation of primary Schwann cell cultures of both ethanol and DMSO, irreversible in a pathological context, after 6 days of treatment [30].

Given the great versatility of curcumin, the limitations of its conventional vehicles, and its low bioavailability, several strategies have emerged to improve its delivery. The use of cyclodextrin/cellulose nanocrystals coated with curcumin [33,34], curcumin in polyethylene glycol [35,36], curcumin nanosuspension in tween 80 [37], curcumin in chitosan/aloe film [38], curcumin conjugated to polyacetal [39], among others [40–42].

Among other alternative approaches, the use of nanoparticles as delivery systems has been shown to be a successful strategy for many compounds [43–45]. Recently, polydopamine (PDA) nanoparticles have been used not only as coatings and surface functionalization[46,47], but also as vehicle [48–52].

Some studies have used PDA to vehicle of curcumin through different approaches. Pan et al. 2020 created carrier-free curcumin nanoparticles of different concentrations between 4 and 50 µg/ml (approximately between 11 µM and 136 µM), which they subsequently coated with PDA, demonstrating that these curcumin-loaded nanoparticles are stable structures, with curcumin release dependent on pH variations [49]. In 2021, Su et al. synthesize PDA nanoparticles, then expose them to curcumin (around 1.13 mM curcumin), demonstrating their antioxidant and antibacterial properties in yeast cultures [50]. Zhao et al., 2022 use PDA nanoparticles coating curcumin loaded with poly L-lactic acid for chemo-photo thermal therapy of osteosarcoma. The work demonstrates that by thermo-activation of nanoparticles loaded with approximately 1 mg/ml curcumin (≃ 2.72 mM), their release in human osteosarcoma cultures (MG-63) is possible, depending on the pH of the intracellular medium [51]. Recently, Lei et al., 2023 coated a rabies virus glycoprotein (RVG29 peptide) to PDA nanoparticles with 0.3 mmol curcumin previously dissolved in PEG and DMSO (approximately 2.24 mM), with the aim of targeting the nanoparticles to the murine brain. The work explores the antiaggregatory effects of curcumin on α-synuclein on different experimental models (Balb/c mice, *C. elegans*, and PC12 cell culture). The results further demonstrate a decrease in oxidative stress levels and apoptosis upon delivery of curcumin through these nanoparticles [52]. The literature thus points to the sensitivity and dependence of curcumin release from PDA nanoparticles in response to the pH of the medium. Likewise, the different effects of curcumin in relation to the dose used, evidence its hormetic action, especially when considering the use of these nanoparticles at the biological level.

In the present work, we propose a new synthesis and loading protocol, using equal concentrations of PDA and curcumin to produce PDA nanoparticles. This protocol incorporates a key dialysis step in order to eliminate possible pH variations outside the

physiological range. We describe the structure of PDA nanoparticles, loaded or not with curcumin, by transmission and scanning electron microscopy. We analyze their loading and unloading dynamics with curcumin, characterizing, the released compounds by UHPLC-MS. Finally, we tested the safety of PDA as a vehicle (without curcumin) and the functional dynamics of nanoparticles loaded with low doses of curcumin in endoneurial fibroblast cultures, evaluating their impact on cell viability and proliferation for prolonged periods of time.

2. Materials and methods

2.1. PDA synthesis and Curcumin loading

Polydopamine nanoparticles (PDA) were polymerized with 10 mM dopamine hydrochloride (Cat#: H8502, Sigma-Aldrich, Taufkirchen, Germany) in TRIS-HCl (Cat#: 1185-53-1, Sigma-Aldrich, Taufkirchen, Germany) buffer pH=8.5, 10 mM, for 12 h at room temperature (RT), protected from light and under constant agitation. Then, a probe sonication was performed, followed by loading with curcumin (10 mM) for 2 h at RT, protected from light and under constant stirring. Dialysis was performed for 12 h at RT, protected from light and under stirring in a 14 kDa membrane (Cat#: D9527, Sigma-Aldrich, Taufkirchen, Germany). Finally, the PDA or Curcumin in PDA (Curc-PDA) was lyophilized for 72 h. The resulting powder was stored at 4°C protected from light until use.

2.2. PDA and Curc-PDA transmission and scanning electron microscopy

The morphology and size of PDA and Curc-PDA in an aqueous solution were determined by transmission electron microscopy (TEM). For unloaded PDA, a suspension of 1.2 mg/ml (10 mM) was made in distilled water, which was then diluted 100-fold (100 µM). For Curc-PDA, the same suspension was made, assuming a similar concentration, of the loaded nanoparticles. A sample drop (10 µl) of PDA or Curc-PDA in distilled water was deposited on a 300-mesh carbon-coated copper mesh, dried for 20 min at RT, and then, the sample was observed by TEM. The surface morphology of PDA and Curc-PDA were also observed by scanning electron microscopy (SEM). Using the same solutions as for TEM, 50 µl was placed in blocks on a double-sided tape, dried at RT, and then metalized for SEB visualization.

2.3. HPLC experiments

2.3.1. UHPLC-MS Analyses

LC-MS analyses were performed by an Ultimate 3000 UHPLC instrument coupled with an ISQ EC mass spectrometer, equipped with an electrospray ion source and a single-quadrupole analyzer (Thermo Fisher Scientific, Cambridge, MA, USA). A C18, Luna® Phenomenex, 5 µm 100 Å (150 × 4.6 mm) (Phenomenex, Torrence, CA, USA) was used for chromatographic separation. The mobile phase was composed of solvents A (Water, 0.1% HCOOH) and B (Acetonitrile, 0.1% HCOOH). An isocratic mode (30:70) was used. The flow rate was set at 0.2 mL/min and the column was maintained at 30 °C for the entire run. Fifty microliters were injected. Analyses were performed using the positive

ionization mode selecting the following m/z: 91, 137, 154, 369. The collision energy (CE) was 20 eV. Mass spectrometry parameters were: spray voltage (V) 3000, sheet gas (arb) 28.8 psig, aux gas (arb) 3.2 psig, ion transfer tube temperature 300 °C, and vaporizer temp 117 °C. Peak areas were measured by using the Chromeleon software (Thermo Fisher Scientific).

2.3.2. Curcumin quantification in PDA

To determine the load of curcumin on PDA nanoparticles, 1 mg/ml solutions of Curcumin alone, unloaded PDA, and Curc-PDA in methanol were created. We then searched for curcumin by UHPLC-MS at m/z=368 ion. We made three independent experiments, with duplicates of each sample. To calculate the curcumin concentration within the PDA; we used the area under the curve of the standard curcumin peak, of known concentration, and obtained the relationship to the area under the curve of the curcumin peak in the Curc-PDA sample.

2.3.3. Release-retention dynamics

To evaluate how curcumin was released from PDA to the culture medium, we studied its release dynamics during 24 h. To do so, we generated a 1 mg/ml solution of Curc-PDA in a culture medium and separated the solution into different tubes to have the samples at different times: 0.5, 1.0, 1.5, 2.0, and 24 h. At each time, the tube was centrifuged, and a sample of the supernatant was taken to look for curcumin released into the culture medium. Then, the medium was removed, replaced by an equal volume of methanol, and centrifuged one more time. As a result, we obtained the curcumin retained in the PDA, which was removed from the nanoparticle by methanol. Both samples were analyzed by UHPLC-MS at m/z=368 ion, in three independent experiments.

2.4. Animals

C57BL wild-type (Wt) mice were obtained from Jackson Laboratories (JAX stock #002504, Jackson Laboratories, Bar Harbor, ME, USA). The colony was maintained at the Clemente Estable Biological Research Institute (IIBCE, MEC) bioterium. The CEUA-IIBCE ethics committee animal approved the experimentation protocol by the No.: 002a/10/2020. Mice were housed in a controlled environment (12 h light/dark cycle) and a mean temperature of 21 ± 3°C with food and water-free access. For this work, postnatal male mice 5 days old (n = 5 for each group) were used.

2.5. Endoneurial fibroblasts' primary culture

Sciatic nerve fibers were dissected as previously described [30]. Briefly, after decapitation, both sciatic nerves were dissected using surgical scissors. The nerves were then immersed in Dulbecco's Modified Eagle's Medium (Cat#: DMEM-HSPTA, Capricorn, Ebsdorfergrund, Germany) supplemented with 10% Bovine Serum (FBS, Cat#: 26140079, Gibco™, Waltham, MA, USA); 5 µg/mL penicillin, 5 µg/mL streptomycin, 10 µg/mL neomycin (PSN 1X, Cat#: 15640055, Gibco™, Waltham, MA, USA). Immediately, the epineurium was removed and the fibers were teased under a stereoscopic microscope.

After, the fibers were incubated for 30 min at 37°C to collagenase (WD: 225 µg/mL, Cat#: C9407, Sigma-Aldrich, Taufkirchen, Germany) in DMEM supplemented, and 5 mM CaCl2. The fibers were centrifugated, the supernatant was removed and it was incubated for 30 min at 37°C to trypsin (WD: 0.25%, Cat#: 15090046, Gibco™, Waltham, MA, USA) in DMEM with PSN 1X. Then, it was centrifugated and finally, the pellet was resuspended in DMEM supplemented, plated, and cultured at 37°C and 5% CO_2. The next days, the culture was evaluated by an inverted light microscope for Schwann cells (SC) and fibroblast (FB) growth. The medium was replaced every 48 h, and after one week, we performed the cold jet procedure [53] to obtain a culture rich in SC and another rich in endoneural fibroblasts. The last one was used in the experiments and was not further than passage 3.

2.6. Determination of the concentration of PDA suitable for cultures

To determine the concentration without effect on the cultures, viability and proliferation assays were performed. The viability of the cultures was studied by 3-(4,5-Dimethylthiazol-2-yl)-2,5 Diphenyltetrazolium Bromide (MTT) assay and the proliferation was carried out with CyQUANT™ Cell Proliferation Assay (Cat#: C7026, Invitrogen, Eugene, OR, USA). For both assays, 1×10^5 cells per well were seeded, in a 96-well plate. 24 h later, the medium was removed and replaced by a medium containing different concentration of PDA (0.32; 0.64; 1.93; 9.63; 19.25; 192.50; 1925 mg/l). The concentrations were evaluated in triplicate and three independent experiments were carried out. The treatment was conducted for five days, with medium changes every 24 h. We used untreated control as a control, being 100% of viability.

Every day, for viability the medium was removed and replaced by culture medium with the reagent MTT (Cat#: M6494, Invitrogen, Eugene, OR, USA), work dilution (WD): 0.5 mg/mL. This pale yellow, water-soluble compound is reduced in the presence of living cells, precipitating as formazan (violet-blue crystals, insoluble in water) [54]. The cells were incubated for 2 h at 37 °C and 5% CO_2. Then, the medium was removed and the cells were lysed with DMSO to release and solubilize the formazan crystals followed by absorbance measurements at 570 nm and 650 nm (background) in the Varioskan® (Varioskan® Flash, Thermo Fisher Scientific, Waltham, MA, USA). For proliferation, each day the medium was removed and replaced by 200 µl of the mixing kit per well, and after 5 min, we performed fluorescence measurements exiting at 480 nm and measuring the emission at 520 nm, in the Varioskan®.

2.7. Treatment with Curc-PDA

To study the effect of curcumin on culture viability and proliferation, a concentration of 0.05 µM curcumin in PDA was used, being below the PDA concentration limit previously determined. Using the same approach as in the previous section, the analysis of MTT and CyQUANT was performed every 24 h, following the effect on the cultures for 5 days. We used PDA without curcumin as a control of 100% of viability and made three independent experiments.

2.8. Statistical Analysis

The normality of the data obtained was evaluated by the Shapiro-Wilk test. The analysis of released and retained compunds was performed with paired student t-test or Wilcoxon test, comparing the values obtained for each time analyzed. Viability and proliferation values for the different PDA concentrations, within each day, were evaluated with one-way ANOVA, with Bonferroni post hoc test, or Kruskal Wallis test, with Dunn's correction. Viability and proliferation values of cultures treated with PDA or with Curc-PDA were evaluated per day, with the unpaired Student's t-test or with the Mann-Whitney test. All tests were applied using a two-tailed distribution and the results were considered significant at an alpha level of 0.05. Statistical analysis was performed with GraphPad Prism version 8.0.0 (RRID: SCR_002798, GraphPad Software, San Diego, CA, USA).

3. Results

3.1. PDA structure and quantification of curcumin loading

The structure of unloaded and curcumin-loaded Polydopamine nanoparticles was determined by Transmission Electron Microscopy (TEM) and Scanning Electron Microscopy (SEM) (Fig. 2A and B). From the images obtained, the diameters of the nanoparticles were calculated. The unloaded PDA showed a diameter of 178±5 nm, while the PDA loaded with curcumin had a diameter of 290±7 nm. The frequency distribution shows the number of nanoparticles in each range, both PDA and Curc-PDA, with a clear area of overlap between these structures (Fig 2C). To determine the amount of curcumin in the PDA, we measured curcumin by UHPLC-MS, releasing it from the PDA by the addition of methanol (Fig.2D). This compound was evaluated at 369 mass-charge-ion (m/z=369), and showed a peak at a retention time of 17.5±0.5 min. Compared with the standard of Curcumin in methanol at the same concentration, we found the concentration of curcumin in the PDA was 0.65±0.04 mg/ml (Fig 2, table), from the curcumin standard and the unloaded PDA control (Table S1).

3.2. Release dynamics of Cruc-PDA in the culture medium

The release dynamics of curcumin were evaluated at different times: 0.5, 1.0, 1.5, 2.0, and 24 h, assessing at each time, the presence of curcumin in the culture medium by UHPLC-MS (Fig. 3). For all times, the release diagrams show the presence of the characteristic peak of curcumin (Fig. 3A in red) at the reported retention time, but also show the presence of a new compound, with the same m/z ratio, but with a shorter retention time, 7.3±0.5 min (Fig. 3A in green), which we will call neo-curcumin. Additionally, the concentrations of curcumin retained in the PDA at different times were measured by UHPLC-MS (Fig. S1). The concentrations obtained from the areas under the curve are visualized in Figure 3C. The released curcumin shows a peak of maximum concentration at 2 h and after 24 h in the medium, it is almost imperceptible. In contrast, neo-curcumin shows a concentration without variations over time, with an average of 17.5±0.4 mg/ml (Fig. 3B left). In the case of retained curcumin, we found that both curcumin and neo-curcumin presented higher concentrations after 24 hours (Fig. 3B right).

3.3. Determination of the PDA no effect concentration in cell cultures

To determine the maximum non-toxic PDA concentration for the cultures, we evaluated two cellular parameters: viability and proliferation (Fig. 4). The cultures were treated with different concentrations of unloaded PDA, ranging from 0.32 mg/l to 1925 mg/l. Based on the previous result of curcumin loading on PDA, these unloaded PDA concentrations allow loading from 0.1 µM to 600 µM curcumin. For each concentration tested, 5 replicates of the culture were generated, to analyze the changes of these cell parameters daily. Those wells that did not receive treatment on that day had their medium changed to the corresponding PDA concentration. The viability was measured with an MTT assay (Fig. 4A). Of the concentrations tested, only 0.32 mg/l was the concentration that showed no difference compared to the control, during the five days of treatment. The rest of the concentrations showed differences on the fifth day of treatment. The proliferation was measured with the CyQUANT assay (Fig 4B). With this assay, we found three concentrations that did not differ from the control, 0.32, 0.64, and 1.93 mg/ml. Since 0.32 was the only concentration that coincided in both parameters, with no toxic effects on the cultures, we decided to continue our evaluation using this concentration of PDA.

3.4. Effects on viability and proliferation of cultures treated with Curc-PDA.

Once the working concentration of PDA was defined as non-toxic to our cultures, we evaluated the effect of curcumin treatment in PDA on the viability and proliferation of the cultures. To be below the established PDA limit, we decided to evaluate the effects of 0.05 µM curcumin (Fig. 5).

In the case of viability, from the second day of treatment, we observed an increase in the number of cells when cultures were treated with Curc-PDA ($p=0.002$), which was maintained on the following days of treatment (day 3: $p=0.002$; day 4: $p=0.001$; day 5: $p=0.04$) (Fig. 5A). If we also evaluated the percentage of accumulated growth, taking as a reference the beginning of the treatment, we find that from the second day onwards all the percentages obtained in cultures treated with Curc-PDA show significant differences with both the control without treatment and the control with unloaded PDA ($p<0.0001$) (Fig. 5C). Comparison of the values obtained with Curc-PDA indicates a significant increase between the first and second day of treatment ($p=0.03$), while between the second, third, fourth, and fifth day, there is no significant difference (Fig. S2A).

The values obtained for proliferation showed an increase in the values with Curc-PDA during the fourth and fifth day of treatment, to the control with unloaded PDA ($p<0.0001$) (Fig 5B). In this sense, the evaluation of cumulative proliferation during the 5 days of treatment also shows an increase in the Curc-PDA treated cultures compared to the negative control and the unloaded PDA control on both the fourth and fifth day (day 4: $p<0.0001$; day 5: $p=0.004$) (Fig. 5D). These results also concur with the comparison of percentages during the whole treatment with Curc-PDA, where an increase of this

parameter is visualized between the third and fourth day (p=0.0002), a difference that is maintained until the fifth day (Fig. S2B).

4. Discussion

We were able to synthesize polydopamine nanoparticles (PDA) and determined 0.32 mg/ml as the maximum concentration of use for our endoneurial fibroblast cultures, with no effect on viability and proliferation. In addition, we loaded the PDA with curcumin, determining the loading concentration and sizes of these loaded and unloaded PDA. After characterization, we evaluated the release of curcumin from PDA in a culture medium, at different times for 24 hours. This allow us to identify that curcumin, detected by UHPLC-MS at a retention time of 17.5 min in the ion m/z=369, has a peak of maximum released at 2 hs, but then its concentration decays, being very low at 24 hs. In parallel, the concentration of curcumin retained in the PDA was also analyzed by UHPLC-MS (Fig. S1 in yellow). At all times analyzed, the concentration of retained curcumin was higher than the released curcumin.

In conjunction with the characterization of curcumin released and retained in the PDA nanoparticles, we detected another peak, at a retention time of 7.3 min. This peak was detected in both the release (Fig 3B in green) and retention analyses (Fig S1 in blue), with concentrations in both cases in the region of 0.15 mg/ml (Fig 3C in green and blue). This peak, which we call neo-curcumin, is not present in the chromatographic profile control only with medium culture, nor with unloaded PDA (1 mg/ml) (Fig. S3). This compound has the same mass charge as curcumin, m/z=369, with the retention time on the column being different. Since neo-curcumin has the same mass, it is possibly a rearrangement or conformational change of the molecule, without chemical changes. It must be a rotamer or tautomer. Based on Chatterjee et al., 2022, one could speculate that we are dealing with a rotamer that allows it to interact less with the resin[55].

To understand where this neo-curcumin peak was coming from, we decided to evaluate the standard of the major degradation product of curcumin, ferulic acid [56,57]. To do so, we studied its ion m/z= 195 and the corresponding curcumin ion (Fig S4). The obtained results for the standard ferulic acid (1 mg/ml in methanol) indicate the presence of a peak at the m/z 369 ion, similar to that found when curcumin is released from PDA.

Curcumin and "neo-curcumin" represent the highest percentage of compounds obtained from curcumin initially loaded on PDA nanoparticles (88.17±1.74 %). We hypothesize that the effects on viability and proliferation observed in cultured endoneurial fibroblasts may be due to these forms of curcumin released from the curc-PDA nanoparticles. We do not rule out the possibility of characterizing the presence of other curcumin derivatives, which, given their low concentration, represent a challenge.

Exposure of cell culture to 0.05 µM curcumin in PDA for 5 days allowed us to observe changes in viability and proliferation (Fig. 5). These changes appeared with a lag time. Still, when they increased, they were maintained over time: while the increase in viability occurred on the second day of treatment, proliferation increased on the fourth

day of treatment (Fig. S2). As the viability assay used is the MTT, the results allow us to consider a scenario in which curcumin initially has an impact at the mitochondrial activity level (or in its modulation), increasing the viability. Subsequently, perhaps the direct action of curcumin and/or the accumulative effect of the mitochondrial implications, changes in proliferation are observed at the end of the treatment. In this regard, mTOR is one of the proteins that connect mitochondrial activity with protein synthesis processes, on which biosynthesis and cell proliferation depend [58]. For this reason, our future work aims to determine the expression of this multiprotein complex to reveal through which mechanisms these processes are connected. Additionally, taking into account the pH dependence that curcumin release has shown in different contexts [49–52], we understand that the incorporation of the dialysis step after the synthesis of curcumin-loaded nanoparticles has resulted in a significant improvement in the quality of the nanoparticles obtained and in their innocuousness as a carrier at the biological level.

Regarding the dose-response phenomena, called hormesis, our results can be classified within the beneficial effects observable at low concentrations of the compound, in this case, curcumin, applied for prolonged periods. This is because there are reports of the use of working concentrations, similar to ours, related to different beneficial effects in cultures: decreases in reactive oxygen species (ROS) [33], increase in members of the chaperone response pathways, autophagy and mTOR [12,30] and cell regeneration increase [59,60]. In contrast, doses in cultures from 40 µm onwards show clear lethal effects, applying curcumin as a potent antitumor [8,20].

Given this broad spectrum of curcumin's action, our main contribution lies in the characterization of a harmless curcumin's vehicle, which guarantees not only that the observed effects can be related to the curcumin and their derivatives supply, but also that they allow a sustained and predictable release over time. Also, our findings contribute to the characterization of nanoparticles as a tool of particular value for in vitro studies focused on the dose/effect relationship over prolonged periods of time, for drug research and therapeutic purposes. In our current approach, it has allowed us to accurately assess the hormetic effect of curcumin.

Acknowledgements: We would like to give special thanks to Dr. Gabriela Casanova, head of the Electron Microscopy Unit of the Facultad de Ciencias de la Universidad de la República, and to her collaborators MSc. Magela Rodao and Dr. Gaby Martínez, for their kind collaboration in the visualization of the nanoparticles by TEM and SEM. We would also like to give special thanks to Dr. Susana Castro head of the Sección Bioquímica of the Facultad de Ciencias de la Universidad de la República and to her collaborator MSc. Celica Cagide, for their kind collaboration in nanoparticles lyophilization. Figure 1 and 3A was created with BioRender.com.

Funding sources: This work was supported by Agencia Nacional de Investigación e Innovación (ANII), Uruguay [grant numbers: FCE_1_2019_1_155539;

POS_NAC_2022_1_173578], the PEDECIBA, CSIC-UdelaR and SNI-ANII. From the Spanish, Ministry of Science and Innovation and the Spanish CIBERNED network [grant PID2019-110401RB-100].

Data Availability Statement: Data available on request due to restrictions e.g., privacy or ethical. The data presented in this study are available on request from the corresponding author.

5. Bibliography

[1] M.A. Tomren, M. Másson, T. Loftsson, H.H. Tønnesen, Studies on curcumin and curcuminoids. XXXI. Symmetric and asymmetric curcuminoids: Stability, activity and complexation with cyclodextrin, Int J Pharm. 338 (2007) 27–34. https://doi.org/10.1016/j.ijpharm.2007.01.013.

[2] J. González-Albadalejo, D. Sanz, J.L. Lavandera, I. Alkorta, J. Elguero, Curcumin and curcuminoids: chemistry, structural studies and biological properties, An. Real Acad. Nac. Farm. 33 (2015) 278–310.

[3] A. Shakeri, A.F.G. Cicero, Y. Panahi, M. Mohajeri, A. Sahebkar, Curcumin: A naturally occurring autophagy modulator, J Cell Physiol. 234 (2019) 5643–5654. https://doi.org/10.1002/jcp.27404.

[4] M.L.A.D. Lestari, G. Indrayanto, Curcumin, in: Profiles Drug Subst Excip Relat Methodol, Academic Press Inc., 2014: pp. 113–204. https://doi.org/10.1016/B978-0-12-800173-8.00003-9.

[5] T.F. Wong, T. Takeda, B. Li, K. Tsuiji, A. Kondo, M. Tadakawa, S. Nagase, N. Yaegashi, Curcumin targets the AKT-mTOR pathway for uterine leiomyosarcoma tumor growth suppression, Int J Clin Oncol. 19 (2014) 354–363. https://doi.org/10.1007/s10147-013-0563-4.

[6] J.L. Mao, X. Xiong, H. Gong, Effects of curcumin on tumor growth and immune function in prostate cancer-bearing mice, Zhonghua Nan Ke Xue. 25 (2019) 590–594. https://europepmc.org/article/med/32223098.

[7] W. Zhang, Q. Li, C. Yang, H. Yang, J. Rao, X. Zhang, Curcumin exerts anti-tumor effects on diffuse large B cell lymphoma via regulating PPARγ expression, Biochem Biophys Res Commun. 524 (2020) 70–76. https://doi.org/10.1016/j.bbrc.2019.12.129.

[8] C.S. Beevers, F. Li, L. Liu, S. Huang, Curcumin inhibits the mammalian target of rapamycin-mediated signaling pathways in cancer cells, Int J Cancer. 119 (2006) 757–764. https://doi.org/10.1002/ijc.21932.

[9] J.S. Wright, Predicting the antioxidant activity of curcumin and curcuminoids, J Mol Struct. 591 (2002) 207–217. https://doi.org/https://doi.org/10.1016/S0166-1280(02)00242-7.

[10] M. Motaghinejad, M. Motevalian, S. Fatima, H. Hashemi, M. Gholami, Curcumin confers neuroprotection against alcohol-induced hippocampal neurodegeneration via CREB-BDNF pathway in rats, Biomedicine and Pharmacotherapy. 87 (2017) 721–740. https://doi.org/10.1016/j.biopha.2016.12.020.

[11] L. Perrone, T. Squillaro, F. Napolitano, C. Terracciano, S. Sampaolo, M.A.B. Melone, The autophagy signaling pathway: A potential multifunctional therapeutic target of curcumin in neurological and neuromuscular diseases, Nutrients. 11 (2019). https://doi.org/10.3390/nu11081881.

[12] S.K. Kang, S.H. Cha, H.G. Jeon, Curcumin-induced histone hypoacetylation enhances caspase-3-dependent glioma cell death and neurogenesis of neural progenitor cells, Stem Cells Dev. 15 (2006) 165–174. https://doi.org/10.1089/scd.2006.15.165.

[13] Y. Peng, M. Ao, B. Dong, Y. Jiang, L. Yu, Z. Chen, C. Hu, R. Xu, Anti-inflammatory effects of curcumin in the inflammatory diseases: Status, limitations and countermeasures, Drug Des Devel Ther. 15 (2021) 4503–4525. https://doi.org/10.2147/DDDT.S327378.

[14] K. Kohli, J. Ali, M.J. Ansari, Z. Raheman, Curcumin: A natural antiinflammatory agent, Indian J Pharmacol. 37 (2005) 141. https://doi.org/10.4103/0253-7613.16209.

[15] A. Barzegar, A.A. Moosavi-Movahedi, Intracellular ROS protection efficiency and free radical-scavenging activity of curcumin, PLoS One. 6 (2011) 1–7. https://doi.org/10.1371/journal.pone.0026012.

[16] M. Caillaud, B. Chantemargue, L. Richard, L. Vignaud, F. Favreau, P.-A. Faye, P. Vignoles, F. Sturtz, P. Trouillas, J.-M. Vallat, A. Desmoulière, F. Billet, Local low dose curcumin treatment improves functional recovery and remyelination in a rat model of sciatic nerve crush through inhibition of oxidative stress, Neuropharmacology. 139 (2018) 98–116. https://doi.org/10.1016/j.neuropharm.2018.07.001.

[17] N. Shinojima, T. Yokoyama, Y. Kondo, S. Kondo, Roles of the Akt/mTOR/p70S6K and ERK1/2 signaling pathways in curcumin-induced autophagy., Autophagy. 3 (2007) 635–7. https://doi.org/10.4161/auto.4916.

[18] F. Forouzanfar, M.I. Read, G.E. Barreto, A. Sahebkar, Neuroprotective effects of curcumin through autophagy modulation, IUBMB Life. 72 (2020) 652–664. https://doi.org/10.1002/iub.2209.

[19] P. Maiti, J. Manna, S. Veleri, S. Frautschy, Molecular chaperone dysfunction in neurodegenerative diseases and effects of curcumin, Biomed Res Int. 2014 (2014). https://doi.org/10.1155/2014/495091.

[20] J. Odot, P. Albert, A. Carlier, M. Tarpin, J. Devy, C. Madoulet, In vitro and in vivo anti-tumoral effect of curcumin against melanoma cells, Int J Cancer. 111 (2004) 381–387. https://doi.org/10.1002/ijc.20160.

[21] H. Abuelba, C.E. Cotrutz, B.A. Stoica, L. Stoica, D. Olinici, T. Petreuş, In vitro evaluation of curcumin effects on breast adenocarcinoma 2D and 3D cell cultures, Romanian Journal of Morphology and Embryology. 56 (2015) 71–76. http://www.rjme.ro/.

[22] A. Turturro, B.S. Hass, R.W. Hart, Does caloric restriction induce hormesis?, Hum Exp Toxicol. 19 (2000) 320–329. https://doi.org/10.1191/096032700678815981.

[23] E.J. Masoro, Role of Hormesis in Life Extension by Caloric Restriction, Dose-Response. 5 (2007) 163-173.0. https://doi.org/10.2203/dose-response.06-005.masoro.

[24] E.J. Calabrese, L.A. Baldwin, Hormesis: The Dose-Response Revolution, Https://Doi.Org/10.1146/Annurev.Pharmtox.43.100901.140223. 43 (2003) 175–197. https://doi.org/10.1146/ANNUREV.PHARMTOX.43.100901.140223.

[25] J.W. Soh, N. Marowsky, T.J. Nichols, A.M. Rahman, T. Miah, P. Sarao, R. Khasawneh, A. Unnikrishnan, A.R. Heydari, R.B. Silver, R. Arking, Curcumin is an early-acting stage-specific inducer of extended functional longevity in Drosophila, Exp Gerontol. 48 (2013) 229–239. https://doi.org/10.1016/j.exger.2012.09.007.

[26] J.L. Watson, R. Hill, P.B. Yaffe, A. Greenshields, M. Walsh, P.W. Lee, C.A. Giacomantonio, D.W. Hoskin, Curcumin causes superoxide anion production and p53-independent apoptosis in human colon cancer cells, Cancer Lett. 297 (2010) 1–8. https://doi.org/10.1016/j.canlet.2010.04.018.

[27] J. Tello Velasquez, M.E. Watts, M. Todorovic, L. Nazareth, E. Pastrana, J. Diaz-Nido, F. Lim, J.A.K. Ekberg, R.J. Quinn, J.A. St John, Low-dose curcumin stimulates proliferation, migration and phagocytic activity of olfactory ensheathing cells, PLoS One. 9 (2014) e111787. https://doi.org/10.1371/journal.pone.0111787.

[28] Z. Zhao, X. Li, Q. Li, Curcumin accelerates the repair of sciatic nerve injury in rats through reducing Schwann cells apoptosis and promoting myelinization, Biomedicine and Pharmacotherapy. 92 (2017) 1103–1110. https://doi.org/10.1016/j.biopha.2017.05.099.

[29] J. Galvao, B. Davis, M. Tilley, E. Normando, M.R. Duchen, M.F. Cordeiro, Unexpected low-dose toxicity of the universal solvent DMSO, FASEB Journal. 28 (2014) 1317–1330. https://doi.org/10.1096/fj.13-235440.

[30] L. Vázquez Alberdi, G. Rosso, L. Velóz, C. Romeo, J. Farias, M.V. Di Tomaso, M. Calero, A. Kun, Curcumin and Ethanol Effects in Trembler-J Schwann Cell Culture, Biomolecules. 12 (2022) 1–19. https://doi.org/10.3390/biom12040515.

[31] S. Adler, C. Pellizzer, M. Paparella, T. Hartung, S. Bremer, The effects of solvents on embryonic stem cell differentiation, Toxicology in Vitro. 20 (2006) 265–271. https://doi.org/10.1016/j.tiv.2005.06.043.

[32] Y. Ilieva, L. Dimitrova, M.M. Zaharieva, M. Kaleva, P. Alov, I. Tsakovska, T. Pencheva, I. Pencheva-El Tibi, H. Najdenski, I. Pajeva, Cytotoxicity and Microbicidal Activity of Commonly Used Organic Solvents: A Comparative Study and Application to a Standardized Extract from Vaccinium macrocarpon, Toxics. 9 (2021) 92. https://doi.org/10.3390/toxics9050092.

[33] M. Caillaud, Z. Msheik, G.M.A. Ndong-Ntoutoume, L. Vignaud, L. Richard, F. Favreau, P.A. Faye, F. Sturtz, R. Granet, J.M. Vallat, V. Sol, A. Desmoulière, F. Billet, Curcumin–cyclodextrin/cellulose nanocrystals improve the phenotype of Charcot-Marie-Tooth-1A transgenic rats through the reduction of oxidative stress, Free Radic Biol Med. 161 (2020) 246–262. https://doi.org/10.1016/j.freeradbiomed.2020.09.019.

[34] G.M.A. Ndong Ntoutoume, R. Granet, J.P. Mbakidi, F. Brégier, D.Y. Léger, C. Fidanzi-Dugas, V. Lequart, N. Joly, B. Liagre, V. Chaleix, V. Sol, Development of curcumin-cyclodextrin/cellulose nanocrystals complexes: New anticancer drug delivery systems, Bioorg Med Chem Lett. 26 (2016) 941–945. https://doi.org/10.1016/j.bmcl.2015.12.060.

[35] C.Y. Kim, N. Bordenave, M.G. Ferruzzi, A. Safavy, K.H. Kim, Modification of curcumin with polyethylene glycol enhances the delivery of curcumin in preadipocytes and its antiadipogenic property, J Agric Food Chem. 59 (2011) 1012–1019. https://doi.org/10.1021/jf103873k.

[36] T. Haukvik, E. Bruzell, S.D. Kristensen, H.H. Tønnesen, Photokilling of bacteria by curcumin in selected polyethylene glycol 400 (PEG 400) preparations: Studies on curcumin and curcuminoids, XLI, Pharmazie. 65 (2010) 600–606. https://doi.org/10.1691/ph.2010.0048.

[37] D. de M. Carvalho, K.P. Takeuchi, R.M. Geraldine, C.J. de Moura, M.C.L. Torres, Production, solubility and antioxidant activity of curcumin nanosuspension, Food Science and Technology (Brazil). 35 (2015) 115–119. https://doi.org/10.1590/1678-457X.6515.

[38] X. Liu, L. You, S. Tarafder, L. Zou, Z. Fang, J. Chen, C.H. Lee, Q. Zhang, Curcumin-releasing chitosan/aloe membrane for skin regeneration, Chemical Engineering Journal. 359 (2019) 1111–1119. https://doi.org/10.1016/j.cej.2018.11.073.

[39] R. Requejo-Aguilar, A. Alastrue-Agudo, M. Cases-Villar, E. Lopez-Mocholi, R. England, M.J. Vicent, V. Moreno-Manzano, Combined polymer-curcumin conjugate and ependymal progenitor/stem cell treatment enhances spinal cord injury functional recovery, Biomaterials. 113 (2017) 18–30. https://doi.org/10.1016/j.biomaterials.2016.10.032.

[40] S.J. Stohs, O. Chen, S.D. Ray, J. Ji, L.R. Bucci, H.G. Preuss, Highly bioavailable forms of curcumin and promising avenues for curcumin-based research and application: A review, Molecules. 25 (2020) 1–12. https://doi.org/10.3390/molecules25061397.

[41] Y. Chen, Y. Lu, R.J. Lee, G. Xiang, Nano encapsulated curcumin: And its potential for biomedical applications, Int J Nanomedicine. 15 (2020) 3099–3120. https://doi.org/10.2147/IJN.S210320.

[42] S.I. Sohn, A. Priya, B. Balasubramaniam, P. Muthuramalingam, C. Sivasankar, A. Selvaraj, A. Valliammai, R. Jothi, S. Pandian, Biomedical applications and bioavailability of curcumin—an updated overview, Pharmaceutics. 13 (2021). https://doi.org/10.3390/pharmaceutics13122102.

[43] K. McNamara, S.A.M. Tofail, Nanoparticles in biomedical applications, Adv Phys X. 2 (2017) 54–88. https://doi.org/10.1080/23746149.2016.1254570.

[44] M. Bilal, Y. Zhao, T. Rasheed, H.M.N. Iqbal, Magnetic nanoparticles as versatile carriers for enzymes immobilization: A review, Int J Biol Macromol. 120 (2018) 2530–2544. https://doi.org/10.1016/j.ijbiomac.2018.09.025.

[45] A. Mokhtarzadeh, A. Alibakhshi, H. Yaghoobi, M. Hashemi, M. Hejazi, M. Ramezani, Recent advances on biocompatible and biodegradable nanoparticles as gene carriers, Expert Opin Biol Ther. 16 (2016) 771–785. https://doi.org/10.1517/14712598.2016.1169269.

[46] M.L. Alfieri, T. Weil, D.Y.W. Ng, V. Ball, Polydopamine at biological interfaces, Adv Colloid Interface Sci. 305 (2022). https://doi.org/10.1016/j.cis.2022.102689.

[47] J. an Li, L. Chen, X. qi Zhang, S. kang Guan, Enhancing biocompatibility and corrosion resistance of biodegradable Mg-Zn-Y-Nd alloy by preparing PDA/HA coating for potential

application of cardiovascular biomaterials, Materials Science and Engineering: C. 109 (2020) 110607. https://doi.org/10.1016/J.MSEC.2019.110607.

[48] J. Liebscher, Chemistry of Polydopamine – Scope, Variation, and Limitation, European J Org Chem. 2019 (2019) 4976–4994. https://doi.org/10.1002/ejoc.201900445.

[49] H. Pan, X. Shen, W. Tao, S. Chen, X. Ye, Fabrication of Polydopamine-Based Curcumin Nanoparticles for Chemical Stability and pH-Responsive Delivery, J Agric Food Chem. 68 (2020) 2795–2802. https://doi.org/10.1021/acs.jafc.9b07697.

[50] R. Su, H. Yan, P. Li, B. Zhang, Y. Zhang, W. Su, Photo-enhanced antibacterial activity of polydopamine-curcumin nanocomposites with excellent photodynamic and photothermal abilities, Photodiagnosis Photodyn Ther. 35 (2021) 1–11. https://doi.org/10.1016/j.pdpdt.2021.102417.

[51] Z. Zhao, S. Chen, Y. Xiao, M. Xie, W. Yu, Supercritical Fluid-Assisted Fabrication of PDA-Coated Poly (l-lactic Acid)/Curcumin Microparticles for Chemo-Photothermal Therapy of Osteosarcoma, Coatings. 12 (2022) 1–14. https://doi.org/10.3390/COATINGS12040524.

[52] L. Lei, Q. Tu, X. Zhang, S. Xiang, B. Xiao, S. Zhai, H. Yu, L. Tang, B. Guo, X. Chen, C. Zhang, Stimulus-responsive curcumin-based polydopamine nanoparticles for targeting Parkinson's disease by modulating α-synuclein aggregation and reactive oxygen species, Chemical Engineering Journal. 461 (2023). https://doi.org/10.1016/j.cej.2023.141606.

[53] C. Mauritz, C. Grothe, K. Haastert, Comparative study of cell culture and purification methods to obtain highly enriched cultures of proliferating adult rat Schwann cells, J Neurosci Res. 77 (2004) 453–461. https://doi.org/10.1002/jnr.20166.

[54] T. Mosmann, Rapid colorimetric assay for cellular growth and survival: Application to proliferation and cytotoxicity assays, J Immunol Methods. 65 (1983) 55–63. https://doi.org/10.1016/0022-1759(83)90303-4.

[55] P. Chatterjee, S.S. Dutta, T. Chakraborty, Tautomers and Rotamers of Curcumin: A Combined UV Spectroscopy, High-Performance Liquid Chromatography, Ion Mobility Mass Spectrometry, and Electronic Structure Theory Study, J Phys Chem A. 126 (2022) 1591–1604. https://doi.org/10.1021/acs.jpca.1c08612.

[56] S. Mondal, S. Ghosh, S.P. Moulik, Stability of curcumin in different solvent and solution media: UV–visible and steady-state fluorescence spectral study, J Photochem Photobiol B. 158 (2016) 212–218. https://doi.org/10.1016/j.jphotobiol.2016.03.004.

[57] L. Shen, H.F. Ji, The pharmacology of curcumin: Is it the degradation products?, Trends Mol Med. 18 (2012) 138–144. https://doi.org/10.1016/j.molmed.2012.01.004.

[58] M. Morita, J. Prudent, K. Basu, V. Goyon, S. Katsumura, L. Hulea, D. Pearl, N. Siddiqui, S. Strack, S. McGuirk, J. St-Pierre, O. Larsson, I. Topisirovic, H. Vali, H.M. McBride, J.J. Bergeron, N. Sonenberg, mTOR Controls Mitochondrial Dynamics and Cell Survival via MTFP1, Mol Cell. 67 (2017) 922-935.e5. https://doi.org/10.1016/j.molcel.2017.08.013.

[59] X. Liu, L. You, S. Tarafder, L. Zou, Z. Fang, J. Chen, C.H. Lee, Q. Zhang, Curcumin-releasing chitosan/aloe membrane for skin regeneration, Chemical Engineering Journal. 359 (2019) 1111–1119. https://doi.org/10.1016/j.cej.2018.11.073.

[60] D. Thaloor, K.J. Miller, J. Gephart, P.O. Mitchell, G.K. Pavlath, Systemic administration of the NF-κB inhibitor curcumin stimulates muscle regeneration after traumatic injury, Am J Physiol Cell Physiol. 277 (1999) C320–C329. https://doi.org/10.1152/ajpcell.1999.277.2.c320.

Figure and legends

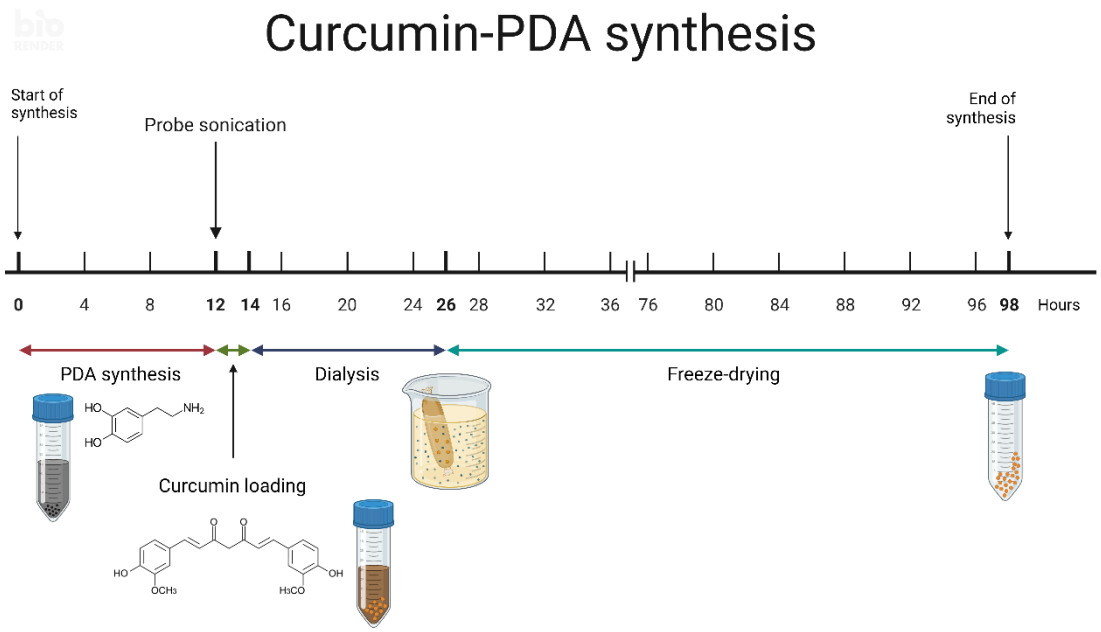

Figure 1. Scheme of PDA synthesis and curcumin loading. Polydopamine (PDA) nanoparticles were polymerized in TRIS-HCl buffer pH=8.5, 10 mM, for 12 h at RT, protected from light and under constant agitation. Then, a stem sonication was performed, followed by loading with curcumin for 2 h at RT, protected from light and under constant stirring. Dialysis was performed for 12 h at RT, protected from light and under constant stirring in a 14 kDa membrane. At the end of the time, the PDA or Curcumin-PDA was lyophilized for 72 hr. The resulting powder is stored at 4°C protected from light until use.

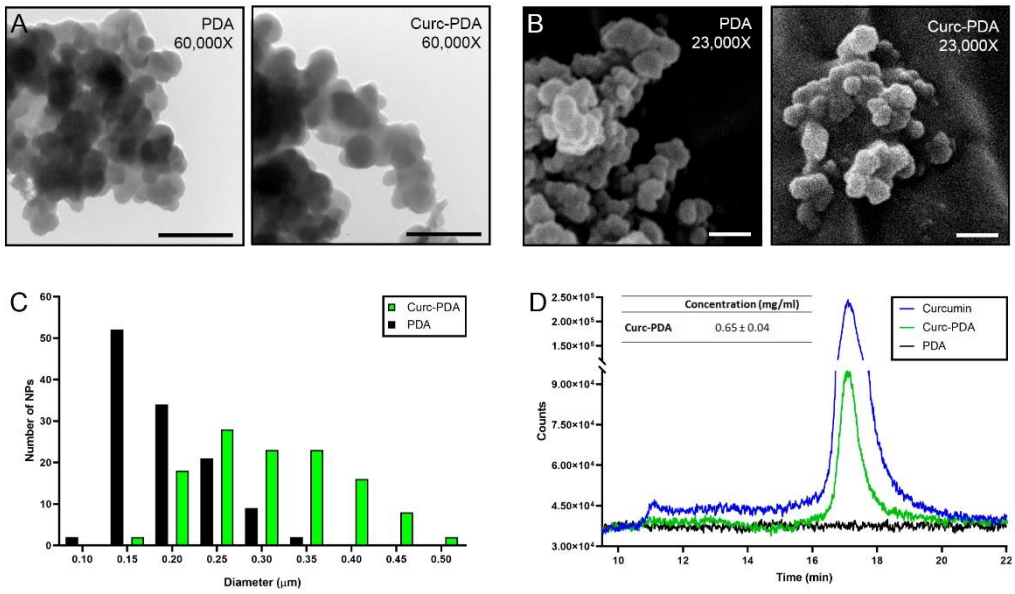

Figure 2. PDA structure and quantification of curcumin loading. A. Transmission electron microscopy images of 100µM unloaded (PDA) and curcumin-loaded (Curc-PDA) NPs. **B.** Scanning electron microscopy images of 100µM PDA and Curc-PDA NPs. **C.** Frequency diagram of the diameters obtained by electron microscopy. **D.** Spectra obtained by UHPLC-MS of samples solubilized in methanol at 1 mg/ml of curcumin, PDA, or Curc-PDA. By area integration, it is obtained that the concentration of curcumin loaded in the NPs expressed as mean ± SEM. Scale: 0.5 µm.

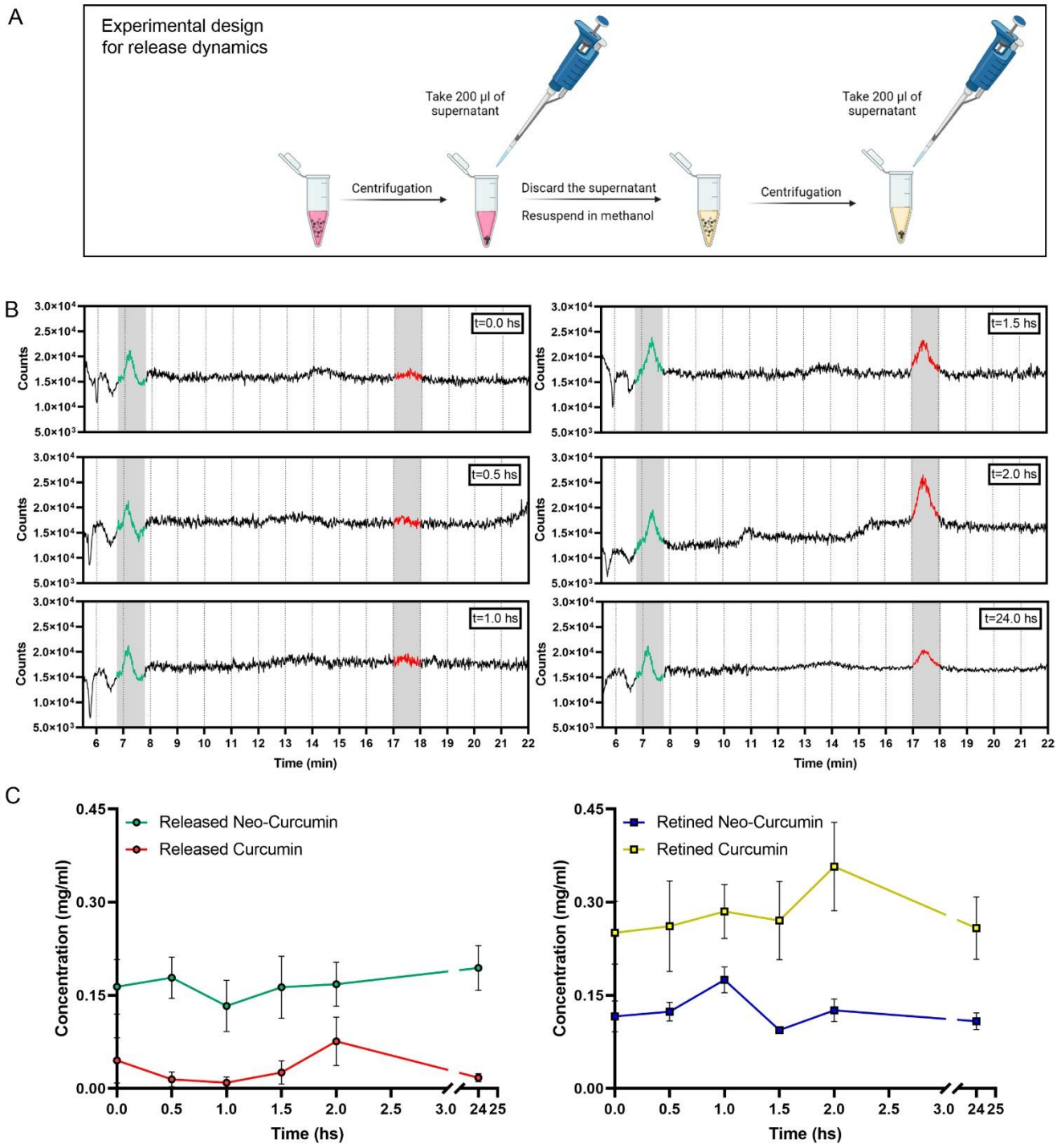

611 **Figure 3. Release dynamics of Cruc-PDA in the culture medium.** Curcumin-loaded NPs were placed in a
612 culture medium, and the presence of curcumin released to the medium and retained in PDA was evaluated
613 after 0.5, 1.0, 1.5, 2.0, and 24 h **A.** Experimental design. **B.** Spectra obtained by UHPLC-MS, m/z=369, for
614 the released curcumin. Red indicates the characteristic peak of curcumin. Green means the presence of a
615 species with the same m/z, detected at all times and in the ferulic acid standard (the latter in Fig. S4),
616 which we call Neo-Curcumin. **C.** Variation of the released and retained concentration and neo-curcumin
617 concentration over time. Each point indicates the mean ± SEM.

618

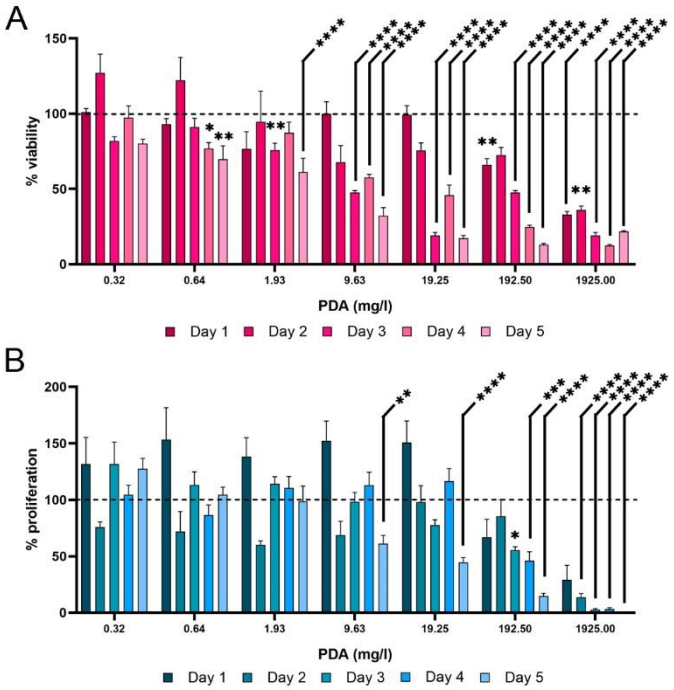

Figure 4. Determination of the no-effect PDA concentration in cell cultures. Before NPs loading, the maximum no-effect PDA concentration on endoneurial fibroblast cultures was determined. During the 5-day treatment, the cultures were tested every day for **A.** Viability (by MTT assay) and **B.** Proliferation (by CyQUANT assay). The graphs show the percentage of the untreated control on the same day. Median ± SIR is plotted.

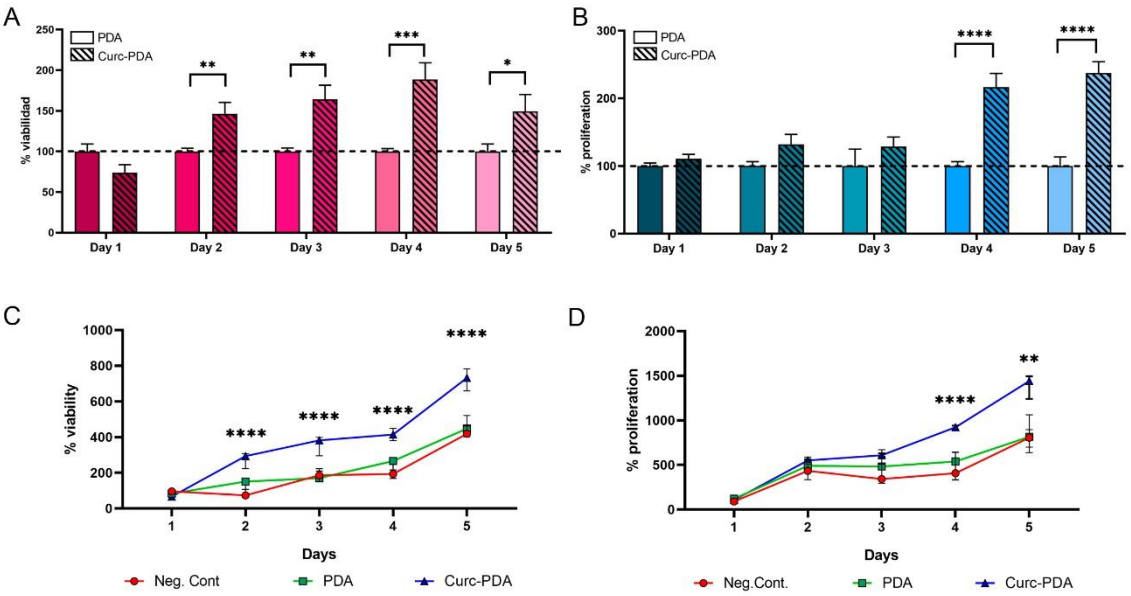

Figure 5. Effects on viability and proliferation of cultures treated with Curc-PDA. Cultures of endoneurial fibroblasts were treated with PDA (0.32 mg/l) and Curc-PDA (0.05µM curcumin) for 5 days, assessing daily: **A.** Viability (by MTT assay) and **B.** Proliferation (by CyQUANT assay). The graphs show the percentage of PDA-treated cultures on the same day. **C.** Cumulative viability. **D.** Cumulative proliferation. Values reported for the first day of treatment D. Median ± SIR is plotted.